

# Functional optimization of electric cell-substrate impedance sensing (ECIS) using human corneal epithelial cells

**Abdul Shukkur Ebrahim**

Wayne State University

**Thanzeela Ebrahim**

Wayne State University

**Hussein Kani**

University of Central Florida

**Ahmed S. Ibrahim**

Wayne State University

**Thomas W. Carion**

Wayne State University

**Elizabeth Berger** (✉ [eberger@med.wayne.edu](mailto:eberger@med.wayne.edu))

Wayne State University

---

## Article

**Keywords:** human corneal epithelial cells (HUCL), ECIS modeling, Rb resistance, alpha resistance, impedance, capacitance, barrier integrity

**Posted Date:** April 8th, 2022

**DOI:** <https://doi.org/10.21203/rs.3.rs-1523126/v1>

**License:** © ⓘ This work is licensed under a Creative Commons Attribution 4.0 International License.

[Read Full License](#)

---

# Abstract

An intact epithelium is key to maintaining corneal integrity and barrier function which can lead to impaired ocular defense and sight-threatening opacity when compromised. Electrical cell-substrate impedance sensing or ECIS is a non-invasive method to measure real-time cellular behaviors including barrier function and cell migration. The current study uses ECIS technology to assess and optimize human telomerase-immortalized corneal epithelial cells (HUCLs) to generate quantifiable measurements that accurately reflect changes in cell behavior in vitro. Five cell densities were assessed in two different media to determine the optimal conditions for monitoring of cellular behavior over time. Parameters of evaluation included: overall impedance ( $Z$ ), barrier resistance ( $R$ ), cell capacitance ( $C$ ), and mathematical modeling of the  $R$  data to further generate  $R_b$  (the electrical resistance between HUCLs),  $\alpha$  (the resistance between the HUCLs and the substrate), and  $C_m$  (the capacitance of the cell membrane) measurements. All parameters of assessment strongly indicated DMEM/F12 at 60,000 cells as the optimal condition for ECIS assessment of HUCLs. Furthermore, this work highlights the ability of the sensitive ECIS biosensor technology to comprehensively and quantitatively assess corneal epithelial cell structure and function and the importance of optimizing not only cell density, but choice of media used for in vitro culturing.

## Introduction

Corneal epithelial cells are widely used for various in vitro assessments, including drug toxicity, host-pathogen interactions, and wound healing. Traditionally, these approaches are limited to cell viability and proliferation rates, cell migration as detected using Boyden chambers and scratch assays, and various secondary measurements (cytokine release, downstream signaling pathways) to represent functional changes. Further, the aforementioned methods tend to lack real-time assessments of changes in cellular structure and function. To this end, we have established the current protocol that optimizes in vitro conditions of human telomerase-immortalized corneal epithelial cells (HUCLs) for analysis using electric cell-substrate impedance sensing or ECIS. This powerful approach is a non-invasive method used to continuously monitor cell behavior and integrity, while dynamically measuring and modeling parameter changes in cell migration and barrier function.

The ECIS system is able to quantify multiple barrier-related parameters to represent changes in cellular behavior over time. This robust functional assessment is possible due to ECIS being an alternating current (AC)-based biosensor that measures impedance ( $Z$ ;  $\Omega$ ), which is comprised of resistance ( $R$ ;  $\Omega$ ) and capacitance ( $C$ ; farad or F)<sup>1</sup>. The use of a constant AC of 1  $\mu$ A with a given frequency as a replacement for a direct current (DC) allows for the separation of overall impedance into overall barrier resistance and cell capacitance<sup>2</sup>. Capacitance measures the overall coverage of the well by the cell layer, whereas resistance is indicative of the barrier function of the epithelial cells<sup>2</sup>. Furthermore, due to the multifrequency nature of ECIS, the impedance data can be mathematically modeled to calculate the intercellular resistance ( $R_b$ ;  $\Omega\text{-cm}^2$ ), the basolateral adhesion of the cells to the substrate ( $\alpha$ ;  $\Omega\text{-cm}^{1/2}$ ), and the capacitance at the cell membrane ( $C_m$ ;  $\mu\text{F}/\Omega\text{-cm}^2$ )<sup>3</sup>. Use of the ECIS system provides a highly

sensitive method to effectively monitor epithelial cell barrier function in a continuous manner and generate quantifiable measurements to evaluate changes in cellular behavior. However, no study to date has utilized the ECIS technology to assess human corneal epithelial cells.

The outermost cornea is a self-renewing, layered epithelial sheet that serves as the primary line of defense against noxious stimuli and invading pathogens. If the epithelial barrier is compromised or suboptimal conditions are present within the corneal microenvironment, pathogenic conditions can develop leading to impaired wound healing and progressive visual opacity<sup>4</sup>. In vitro representation of an intact epithelium is integral to studying corneal homeostasis and pathogenic events associated with disease. To this end, human corneal epithelial cell lines are often used and are traditionally grown in keratinocyte serum-free medium (K-SFM) as a standard<sup>5</sup>. These cells effectively represent the apical layer of nonkeratinized squamous cells that form tight junctions between adjacent cells and regulate the passage of molecules, toxins, and fluids in the cell environment<sup>6</sup>. Therefore, the current study sought to optimize growth conditions as assessed by ECIS biosensor technology using HUCLs at different cell densities and culture media. Quantifiable measurements were generated that accurately reflect changes in cell behavior under in vitro conditions. The ECIS assessments provide critical insights into: (1) how long it takes for the epithelial cells to spread and form a confluent monolayer; (2) when the epithelial barrier has formed; (3) when the epithelial barrier is the strongest; (4) contribution of paracellular barrier ( $R_b$ ) to overall resistance; and (5) contribution of basal adhesion ( $\alpha$ ) to overall resistance. Furthermore, we provide clear ECIS-derived evidence that DMEM/F12 media supplemented with 10% FBS is ideal for HUCL growth, attachment, spreading, and barrier formation as opposed to the traditionally used non-supplemented K-SFM media.

## Results

### *Three-dimensional bio-impedance analysis*

Bio-impedance analysis of HUCLs was carried out to compare two different cell culture media (DMEM/F12 and K-SFM) at three different cell densities (30,000, 60,000 and 100,000 cells per well) as shown in **Figure 1 (A – F)**. HUCLs formed a mature confluent barrier as indicated by a plateau in the impedance ( $Z$ ) represented as log normalized values on the y-axis in the 3D model. As such, HUCLs grown in DMEM/F12 media at all three seeding densities (**A – C**) formed a mature confluent barrier faster than similar cells grown in K-SFM media (**D – F**). Furthermore, three-dimensional representations of normalized impedance across HUCLs as a function of both time and log frequency showed DMEM/F12 at a density of 60,000 was most optimal for barrier maturation (**B**). Likewise, at a 60,000-seeding density, the logarithmic growth curve reached a plateau (time to confluency) after 6 hours with DMEM/F12 (**B**) compared to >14 hours with K-SFM (**E**). Thus, indicating that HUCLs grown in the supplemented media more efficiently form an epithelial barrier than cells similarly grown in unsupplemented media.

Next, we aimed to dissect the influence of DMEM/F12 and K-SFM media on the two components of impedance: pure resistance ( $R$ ) and capacitance ( $C$ ). When cells are challenged with an AC, both  $R$  and  $C$

are created, resulting in the overall impedance,  $Z$ . To determine which frequency to use in subsequent evaluations, frequency dependence spectra of these parameters were measured as shown in **Figure 2**. The frequency dependence of variables  $Z$ ,  $R$ , and  $C$  for cells grown in DMEM/F12 at the three cell densities at  $T = 15$  hours are shown in panels **A – C**, respectively. Panels **D – F** display the same information for HUCLs grown in K-SFM at  $T = 15$  hours. As shown in **Figure 2**, the impedance spectrum showed a characteristic frequency of 32 kHz, providing the greatest possible range for group comparison of cells grown in DMEM/F12 (**A**) and K-SFM media (**D**). On the other hand, we observed that 4000 Hz produces the maximum resistance in both DMEM/F12 and K-SFM media (**Fig. 2B & E**, respectively). Further, capacitance ratios displayed that optimal cell spreading was achieved at 64 kHz for both DMEM/F12 (**Fig. 2C**) and K-SFM media (**Fig. 2F**). However, K-SFM showed overlap between the three cell densities with greater standard deviations than DMEM/F12, thus indicating potential suboptimal conditions for HUCLs growing in the K-SFM media.

### *Impedance measurements*

Impedance (capacitive reactance) measurements, as shown in **Figure 3A – E**, calculated at a high frequency provide information as to when the cell monolayer is in place and confluent. This is reflected by the plateau in the impedance when measured at 32 kHz. Cells grown in DMEM/F12 reached the plateau phase at 15 hours for the 30,000-seeding density, and at 4 – 6 hours for both 60,000- and 100,000-seeding densities. Whereas HUCLs seeded at the same densities but grown in K-SFM did not display a distinct plateau phase, indicative of poor HUCL spreading. This trend is further illustrated in both total (**Fig. 3D**) and endpoint (**Fig. 3E**) impedance measurements generated at 32 kHz; impedance values for HUCLs grown in DMEM/F12 were significantly higher when compared to K-SFM media. These impedance measurements indicate that the HUCLs grown in the DMEM/F12 are able to form and maintain a strong and confluent monolayer. Thus, indicating that investigation of HUCL barrier formation should be carried out using supplemented DMEM/F12 media in place of the classically used K-SFM media.

### *Resistance measurements*

Resistance measurements taken at a low frequency provides insight into the barrier formation and function. **Figure 4A – C** show resistance measurements generated at 4000 Hz from HUCLs seeded at the three different cell densities and grown in the two different culture media. Barrier formation is indicated by the plateau phase in each resistance profile. HUCLs grown in supplemented DMEM/F12 reached the highest resistance (9,000  $\Omega$ ) at 60,000 (**B**) and 100,000 (**C**) seeding densities. However, HUCLs cultured in K-SFM failed to reach a distinct “plateau phase” with a maximum resistance of  $\sim 6,000 \Omega$ . The total and endpoint resistance values shown in **Figure 4D** and **E**, respectively, were generated out to a maximum of 16 hours as determined by the barrier formation plateaus for both groups of media. Total resistance values were significantly higher in DMEM/F12 versus K-SFM at seeding densities of 60,000 and 100,000 cells. Furthermore, endpoint resistance measurements showed that all three cell densities grown in DMEM/F12 were significantly higher compared to K-SFM cells, indicating the formation of tighter and

stronger epithelial cell barriers when grown in DMEM/F12. Collectively, these results indicate that the optimal growth, barrier formation, and sustaining conditions for HUCLs are best carried out in the DMEM/F12 media. Without the supplementation, as indicated by HUCLs grown in K-SFM, “mature” barriers are not formed, thus providing further evidence for the use of supplemented DMEM/F12 media when studying corneal epithelial function in vitro.

### *Capacitance measurements*

As with the resistance measurements described above, the growth characteristics of HUCLs were observed in the real-time formation of confluent cell layers and measured as capacitance (**Fig. 5A – E**). Cells grown in the supplemented DMEM/F12 media displayed more efficient cell spreading at all seeding densities compared to cells grown in K-SFM. At the 30,000 seeding cell density (**A**), cells grown in DMEM/F12 reached a confluent monolayer between 12 and 14 hours. HUCLs seeded at 60,000 and 100,000 cells grown in the DMEM/F12 formed a confluent monolayer between 2 – 4 hours (**B & C**). Whereas HUCLs at either 30,000 or 60,000 seeding densities grown in K-SFM exhibited much less efficient cell spreading. Cells grown in K-SFM were able to establish a confluent layer; however, it took much longer at 15 hours. To further illustrate the differences between DMEM/F12 and K-SFM in the formation of a confluent layer, total and endpoint capacitance measurements are also shown. Total capacitance (**Fig. 5D**) was significantly lower at 60,000 and 100,000 cell seeding densities for DMEM/F12 compared to K-SFM. As shown in **Figure 5E**, endpoint capacitance for all three seeding densities was significantly decreased in DMEM/F12, as well. Because of the inverse relationship between capacitance and cell spreading, it is indicated that the DMEM/F12 media better supports the growth, spreading and formation of a confluent cellular layer compared to the classically used K-SFM growing conditions.

### *Mathematical modeling of the R data - $R_b$ , $\alpha$ and $C_m$*

The ECIS software has the ability to model the impedance into parameters that distinguish between cell-cell ( $R_b$ ) and cell-matrix ( $\alpha$ ) adhesions, as well as membrane capacitance ( $C_m$ ).  $R_b$  is the resistivity of cell-cell contacts to the current flow.  $\alpha$  is measures the impedance contributions arising from the cell-electrode junctions. Therefore, the contribution of  $R_b$ ,  $\alpha$ , and  $C_m$  to the observed changes in previous experiments was calculated by fitting a mathematical model developed by Giaever and Keese<sup>7</sup>.  $R_b$ ,  $\alpha$ , and  $C_m$  values were measured from HUCLs at the 60,000 cell seeding density grown in DMEM/F12 compared to K-SFM media and are presented in **Figure 6A–F**.

The constructed parameter  $\alpha$ , indicating the strength of interaction between the cells with the basal substrate, is higher in cells grown in DMEM/F12 compared to K-SFM throughout the entire time course (**Fig. 6A**). These results combined with total and endpoint  $\alpha$  measurements (**Fig. 6D**), which are also significantly higher for HUCLs grown in DMEM/F12 compared to K-SFM, indicate that cells grown in the DMEM/F12 media create stronger cellular attachments to the basal substrate. These data may also contribute to the overall differences seen in the resistance values between HUCLs grown in DMEM/F12 versus K-SFM.

Furthermore,  $R_b$  values, which is indicative of paracellular barrier strength, were higher in HUCLs cultured in DMEM/F12 media when compared to HUCLs grown in K-SFM media (**Fig. 6B**). This observed increase in barrier function is further demonstrated by corresponding total and endpoint  $R_b$  values (**Fig. 6E**), where HUCLs grown in DMEM/F12 displayed significantly higher  $R_b$  values than K-SFM media. In addition to the  $\alpha$  value, the fact that HUCLs grown in DMEM/F12 displayed higher  $R_b$  values compared to the cells grown in K-SFM indicates the stronger cell-cell interactions are also playing an underlying role in the overall differences observed in resistance.

$C_m$ , or the capacitance of the cell membrane, is indicative of temporal alterations in membrane thickness and composition, as shown in **Figure 6C**. Additionally,  $C_m$  measurements are used to determine if variations in capacitance are only due to changes in electrode coverage or are a function of microvariations in the apical membrane structures. Total  $C_m$  is not presented since confluent monolayers are required to model this parameter, which did not consistently occur at earlier timepoints for cells grown in K-SFM. As a result, only end-point  $C_m$  is shown, which is significantly lower in HUCLs grown in DMEM/F12 compared to K-SFM (**Fig. 6F**). Therefore, the interpretation from the data is that the differences in  $C_m$  are due to differences in electrode coverage and not membrane structure.

## Discussion

The ECIS biosensor technology is a powerful tool to measure and model key aspects of cellular function that provide insight into changes in cellular structure. The current study highlights the comprehensive analyses generated by ECIS for in vitro study of human corneal epithelial cells. These quantitative assessments directly relate to cellular function, particularly spreading and barrier formation, which are key to maintaining corneal homeostasis as well as contributing factors to disease pathogenesis. Taken together, real-time measurements of parameters that include impedance ( $Z$ ), resistance ( $R$ ), capacitance ( $C$ ),  $R_b$ ,  $\alpha$ , and  $c_m$  allow for a more extensive understanding regarding the structural and functional aspects of a cell under in vitro conditions than more traditional techniques that are standardly used.

Real-time impedance ( $Z$ ) measurements are indicative of cellular motility and the rate at which the corneal epithelial barrier is formed. Impedance is then broken down into resistance ( $R$ ) and capacitance ( $C$ ) to allow for differentiation of adhesion, spreading, and proliferation – a major limitation to traditional in vitro approaches<sup>8</sup>. Resistance is the part of impedance that best defines barrier quality and function because it does not consider capacitive components from the membrane, electrode or cell medium<sup>9</sup>. Resistance itself is directly determined by the cell through cell-cell and cell-substrate interactions that block the flow of current. When cells attach to the substrate, for example, the flow of current will become increasingly restricted as the cells spread over the electrode. As a result, at higher frequencies, the capacitance decreases in a linear correlation to the percentage of open electrode area<sup>8</sup>. In this case, adhesion, spreading and proliferation are quantified at a frequency higher than 40 kHz. Complete cellular coverage of the electrode is indicated by the flattening out of the slope related to the capacitance curve. It is important to underscore that capacitance measurements indicate coverage, but resistance data reveal

when a mature barrier is formed. To this end, we show that HUCLs grown in DMEM/F12 generated a confluent monolayer between 2 – 3 hours (indicated by capacitance), but a functional barrier was not established until 4 – 6 hours (indicated by resistance). This highlights the power of ECIS in allowing for a more accurate interpretation of cellular changes, while also calling attention to the importance of precise data interpretation.

Impedance measurements acquired across several frequencies can be mathematically modeled using the ECIS software to obtain important parameters that together relate to the overall barrier formation of these cells. These values are  $R_b$  (resistance of the paracellular barrier),  $\alpha$  (resistance of the cell:substrate barrier) and  $c_m$  (capacitance of the cell membrane). ECIS is the only impedance measuring system to use multifrequency AC currents, which results in more robust data compared to systems like xCELLigence by ACEA, which only generates data from a single AC frequency<sup>10</sup>. Separating cell-cell ( $R_b$ ) adhesions from cell-substrate ( $\alpha$ ) interactions provide key insights into understanding which elements of the corneal epithelial barrier are contributing to the overall barrier strength and resistance.  $R_b$  is the resistivity of cell-cell contacts to the current of flow. As a result, high  $R_b$  implies a low permeability towards the current flow and thus stronger cell-cell adhesions. Alpha ( $\alpha$ ) is a measure for the impedance contributions that arise from the cell-substrate junctions. The model to quantify cell-cell and cell-substrate contacts was introduced in 1991 by Giaever and Keese and assumes that cells are circular, disc-shaped objects that have an insulating membrane, hover over the electrode, and are filled with a conducting electrolyte<sup>7</sup>.

Our study first aimed to determine the experimental parameters (media type, supplementation details, seeding densities, and frequency range) that would allow for optimal in vitro assessment of corneal epithelial cell function using the ECIS system. Previous in vitro studies investigating corneal epithelial cells have used serum-containing media and others have used serum-free media. The reason being that serum may influence the proliferation and differentiation of corneal epithelial cells<sup>11</sup> since it may contain growth factors that unknowingly inhibit or activate cellular growth. Our ECIS studies were initially carried out using the traditional corneal epithelial cell media, K-SFM for the reason stated above. However, extreme variations in the data were consistently observed and surprisingly weak readings for impedance, resistance and capacitance were generated for HUCLs compared to other studies looking at epithelial cell barrier formation. We had previously published on ECIS assessment of the human retinal pigment epithelial cell line, ARPE-19, which is widely used as an alternative for primary retinal pigment epithelial cells. This cell line is grown in DMEM/F12 medium as a standard<sup>12,13</sup>. Further, the literature revealed studies of different types of epithelial cells (retinal epithelial cells<sup>12</sup> and kidney epithelial cells<sup>14</sup>) also utilized DMEM/F12 media supplemented with 10% FBS. Therefore, we compared both K-SFM media with no FBS supplementation and supplemented DMEM/F12.

HUCLs maintained in DMEM/F12 media were found to outperform cells similarly grown in K-SFM across all parameters. This was evidenced by real-time impedance (Z) measurements indicating faster barrier formation and better motility. Not only did these cells migrate more quickly but they also formed a stronger corneal epithelial barrier than cells grown in K-SFM media. Resistance measurements taken from

DMEM/F12 were almost 2× greater than that observed in K-SFM. In addition, a corneal epithelial barrier was established in ~1/3 of the time it took for cells grown in K-SFM, as indicated by the R plateau. In fact, no true R plateau, indicating formation of a functional barrier, was observed in the latter group by the 15 hour endpoint. Capacitance data reveal correlative findings where cells grown in DMEM/F12 formed a monolayer in 2 – 3 hours compared to 15+ hours for cells grown in K-SFM. Furthermore, the slope of the capacitance curve is much steeper for HUCLs grown in DMEM/F12 compared to K-SFM, reflecting cells that are much more motile and spread more quickly across the area of the electrode. Not surprisingly, HUCLs grown in DMEM/F12 also had stronger cell-cell ( $R_b$ ) and cell-substrate ( $\alpha$ ) interactions than cells grown in K-SFM. These data reveal that the differences in  $R_b$  and  $\alpha$  are the underlying reasons for such drastic differences in the resistance and capacitance readings between the two groups of media. HUCLs grown in DMEM/F12 are able to form stronger tight junctions between neighboring cells and also create stronger interactions with the basal substrate. Thus, it appears that DMEM/F12 provides essential nutrients needed to migrate efficiently and form a strong and tight corneal epithelial cell barrier under in vitro conditions. This is significant because previously, K-SFM was thought to be the ideal culture medium standard for corneal epithelial cells. However, as observed using the ECIS system, these cells demonstrate poor cell migration and reduced barrier formation in K-SFM media.

As shown, 60,000 cells per well generated the optimal data for HUCLs. Seeding densities >100,000 cells were also evaluated and are included as **Supplemental Data**, which resulted in barrier function stress and greater standard deviations for impedance, resistance, and capacitance parameters. This work also highlights the sensitivity of the ECIS technology and the importance of optimizing for cell density.

In conclusion, our study provides a first account of using ECIS to monitor cellular behavior in HUCL cells, while optimizing cell culturing conditions in vitro. Without a comprehensive assessment of cellular behavior in real-time, it is likely that traditional in vitro conditions may miss the mark regarding growing conditions. The current study not only highlights the importance of optimization but also data interpretation. For example, assuming that a confluent monolayer equates to a functional barrier regarding the latter point. In future studies, ECIS will be utilized to measure corneal epithelial wound healing migration and subsequent re-establishment of a mature epithelial barrier. Additionally, this approach can be used to evaluate the functional influence of potential therapies being developed for microbial keratitis or dry eye disease. Collectively, the ECIS system provides a valuable opportunity to elucidate cellular migration and mature barrier formation in vitro.

## Materials And Methods

### *Human telomerase-immortalized corneal epithelial cell (HUCL) culture*

HUCLs, kindly provided by Dr. Fu-Shin Yu's laboratory, were used in these studies. These cells, infected with a retroviral vector encoding human telomerase reverse transcriptase to create an immortalized cell line, have been previously described and appropriately confirmed as an applicable in vitro model for corneal epithelial cell investigation<sup>15</sup>. In the current study, HUCLs were maintained in two different media

for all experiments: Dulbecco's modified Eagle's medium–nutrient mixture F12 (DMEM/F-12; Thermo Scientific, Wyman, MA, USA) supplemented with 10% fetal bovine serum (FBS; Atlantic Biological, Norcross, GA, USA) and 1% penicillin/streptomycin (PS) and keratinocyte-serum-free medium (K-SFM) supplemented with growth factors (EGF and bovine pituitary extract; Invitrogen-Life Technologies, Carlsbad, CA, USA). Cells were used between passages 3 – 5 for all experiments and maintained in a humidified 5% CO<sub>2</sub> incubator at 37°C.

### *Conducting ECIS experiments and modeling*

HUCL assessments were determined by observing changes in transcellular electrical resistance (TER) using the ECIS Z $\Theta$  system (Applied Biophysics Inc, Troy, NY, USA)<sup>12</sup>. Electrode arrays (96W20idf) (Applied Biophysics Inc., Troy, NY, USA) are 96-well plates with each well containing an electrode with an interdigitated finger configuration. The total area of the electrode is 3.985 mm<sup>2</sup>. Arrays were pretreated with 100  $\mu$ L of 100  $\mu$ M cysteine for 30 minutes, followed by coating with fibronectin collagen (FNC Coating Mix; Athena Environmental Service, Inc., Baltimore, MD, USA) for 2 minutes. Prior to seeding the wells, electrode impedance values were stabilized, as recommended by the manufacturer, to minimize electrode drift during the experiment. Wells were then inoculated with HUCLs at five different seeding densities: 30,000, 60,000, 100,000, 200,000 and 500,000 cells per well in 200  $\mu$ L of media. The plate was maintained for ~15 hours at a constant current of approximately 1  $\mu$ A to each well. The run was carried out under multiple frequencies ranging from 1000 Hz – 64 kHz and continuously monitored with measurements taken roughly every 2 minutes. Impedance values were normalized to the impedance values generated by cell-free electrodes. ECIS measurements were acquired from five replicates per experiment.

### *Data analysis and modeling*

ECIS measurements were acquired for overall resistance (R), impedance (Z), and capacitance (C) at 4 kHz, 32 kHz and 64 kHz, respectively, as a function of time. Parameters were determined by comparing cell data to cell-free electrodes, per the manufacturer's recommendation. Multi-frequency scans were used to measure impedance also as a function of frequency and represented as a three-dimensional plot with frequency along the x-axis and time along the z-axis.

The ECIS technology is enhanced by the ability to apply mathematical modeling to derive three parameters that reflect the properties of cells:  $R_b$  (the electrical resistance between cells,  $\Omega$ -cm<sup>2</sup>),  $\alpha$  (the basolateral resistance between the HUCLs and substrate,  $\Omega$  -cm<sup>1/2</sup>), and  $c_m$  (the capacitance of the HUCL cell membrane,  $\mu$ F/cm<sup>2</sup>). The ECIS software was also used to model these parameters as total and end point values as previously described<sup>2</sup>. The parameter  $R_b$  is crucial to modeling in vitro epithelial barrier function, as it describes the tightness of the intercellular space, which is highly dependent on cell-cell junctions. The two remaining parameters,  $\alpha$  and  $c_m$ , are indicative of the current flow below or through cells, respectively. ECIS biosensor technology is the only technology currently available that can model each of these important cellular parameters. However, average capacitance of cell membranes cannot

distinguish between apical and basal membranes. Drift Correction and Model Fit RMSE (root mean square error) values were used to validate the modeled data.

### *Statistical analysis*

Each experiment was repeated at least five times and statistical analyses were performed using GraphPad Prism 7.03. Data are presented as mean  $\pm$  SEM for one representative experiment. Differences between multiple groups were determined by a two-way ANOVA with multiple comparisons (main mean effect). Comparisons made between two groups were made using an unpaired, Student's t-test. Significance was determined by p-values  $< 0.05$  and represented as follows: \* $p < 0.05$ , \*\* $p < 0.01$ , \*\*\* $p < 0.001$ .

## Declarations

### Authors' Contributions Statement

A.S.E. performed experiments, collected data and wrote the manuscript. T.W.C. contributed to data analysis and wrote the manuscript. T.E. and H.K. contributed to data analyses. A.S.I. contributed to data analysis. E.A.B. designed the studies, edited the manuscript, and funded the work. All authors have read and approved of this manuscript.

### Competing Interests Statement

The authors declare that they have no competing interests.

### Data Availability Statement

All data generated during and/or analysed during the current study are included in this published article.

**Grant funding:** NIH NEI R01EY029836 (EAB), American Heart Association (AHA) 18CDA34080403 (ASI), Eversight Center for Vision and Eye Banking Research, Research to Prevent Blindness (RPB), NIH NEI P30EY004068 (Core Grant)

## References

1. Reiss, B. & Wegener, J. Impedance analysis of different cell monolayers grown on gold-film electrodes. *Annu Int Conf IEEE Eng Med Biol Soc* **2015**, 7079-7082, doi:10.1109/EMBC.2015.7320023 (2015).
2. Robilliard, L. D. *et al.* The Importance of Multifrequency Impedance Sensing of Endothelial Barrier Formation Using ECIS Technology for the Generation of a Strong and Durable Paracellular Barrier. *Biosensors (Basel)* **8**, doi:10.3390/bios8030064 (2018).
3. Stolwijk, J. A., Matrougui, K., Renken, C. W. & Trebak, M. Impedance analysis of GPCR-mediated changes in endothelial barrier function: overview and fundamental considerations for stable and

- reproducible measurements. *Pflugers Arch***467**, 2193-2218, doi:10.1007/s00424-014-1674-0 (2015).
4. Stepp, M. A. & Menko, A. S. Immune responses to injury and their links to eye disease. *Transl Res***236**, 52-71, doi:10.1016/j.trsl.2021.05.005 (2021).
  5. Li, H.*et al.* Herpes simplex virus 1 infection induces the expression of proinflammatory cytokines, interferons and TLR7 in human corneal epithelial cells. *Immunology***117**, 167-176, doi:10.1111/j.1365-2567.2005.02275.x (2006).
  6. Sridhar, M. S. Anatomy of cornea and ocular surface. *Indian J Ophthalmol***66**, 190-194, doi:10.4103/ijo.IJO\_646\_17 (2018).
  7. Giaever, I. & Keese, C. R. Micromotion of mammalian cells measured electrically. *Proc Natl Acad Sci U S A***88**, 7896-7900, doi:10.1073/pnas.88.17.7896 (1991).
  8. Wegener, J., Keese, C. R. & Giaever, I. Electric cell-substrate impedance sensing (ECIS) as a noninvasive means to monitor the kinetics of cell spreading to artificial surfaces. *Exp Cell Res***259**, 158-166, doi:10.1006/excr.2000.4919 (2000).
  9. Szulcek, R., Bogaard, H. J. & van Nieuw Amerongen, G. P. Electric cell-substrate impedance sensing for the quantification of endothelial proliferation, barrier function, and motility. *J Vis Exp*, doi:10.3791/51300 (2014).
  10. Kho, D.*et al.* Application of xCELLigence RTCA Biosensor Technology for Revealing the Profile and Window of Drug Responsiveness in Real Time. *Biosensors (Basel)***5**, 199-222, doi:10.3390/bios5020199 (2015).
  11. Kruse, F. E. & Tseng, S. C. Serum differentially modulates the clonal growth and differentiation of cultured limbal and corneal epithelium. *Invest Ophthalmol Vis Sci***34**, 2976-2989 (1993).
  12. Guerra, M. H.*et al.* Real-Time Monitoring the Effect of Cytopathic Hypoxia on Retinal Pigment Epithelial Barrier Functionality Using Electric Cell-Substrate Impedance Sensing (ECIS) Biosensor Technology. *Int J Mol Sci***22**, doi:10.3390/ijms22094568 (2021).
  13. Ahmado, A.*et al.* Induction of differentiation by pyruvate and DMEM in the human retinal pigment epithelium cell line ARPE-19. *Invest Ophthalmol Vis Sci***52**, 7148-7159, doi:10.1167/iovs.10-6374 (2011).
  14. Lo, C. M., Keese, C. R. & Giaever, I. Impedance analysis of MDCK cells measured by electric cell-substrate impedance sensing. *Biophys J***69**, 2800-2807, doi:10.1016/S0006-3495(95)80153-0 (1995).
  15. Zhang, J.*et al.* Role of EGFR transactivation in preventing apoptosis in *Pseudomonas aeruginosa*-infected human corneal epithelial cells. *Invest Ophthalmol Vis Sci***45**, 2569-2576, doi:10.1167/iovs.03-1323 (2004).

## Figures

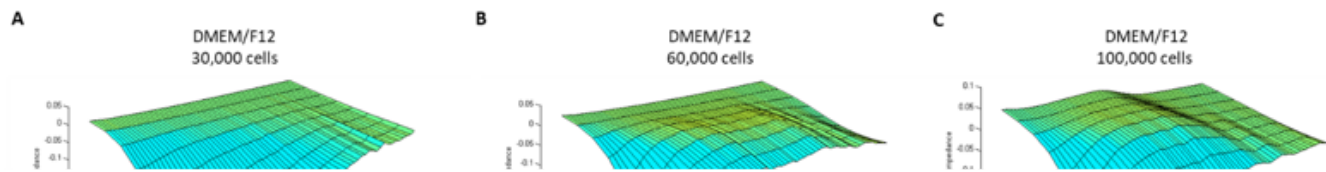


**Figure 1**

Barrier function of HUCLs monitored by real-time bio impedance analysis. HUCLs were seeded at 30,000, 60,000 and 100,000 cells per well on a 96W20idf ECIS array. Three-dimensional representations of the log of normalized impedance (y-axis) as a function of both log frequency of the alternating-current (AC) (x-axis) and time (z-axis). Cells grown in DMEM/F12 and K-SFM are shown for 30,000 (**A, D**), 60,000 (**B, E**) and 100,000 (**C, F**) cell seeding densities. Arrows indicate start of plateau.

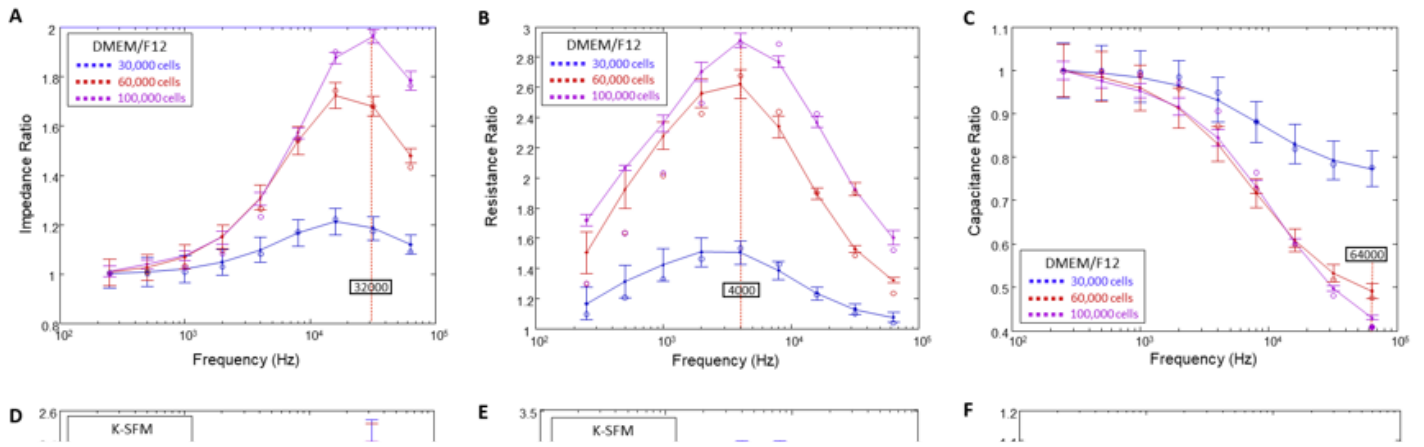


**Figure 2**

Separation of impedance into resistance and capacitance. Impedance ratio of cell-free medium versus frequency (Hz) measured at 15 hours in HUCLs grown in DMEM/F12 (**A**) and K-SFM (**D**), with a local maximum at 32 kHz. Resistance ratio of cell-free medium versus frequency (Hz) measured at 15 hours in HUCLs grown in DMEM/F12 (**B**) and K-SFM (**E**), with a maximum at 4000 Hz. Capacitance ratio versus frequency (Hz) measured at 15 hours in HUCLs grown in DMEM/F12 (**C**) and K-SFM (**F**), with a local minimum at 64 kHz. Data shown are the mean  $\pm$  SEM; n = 5/group.

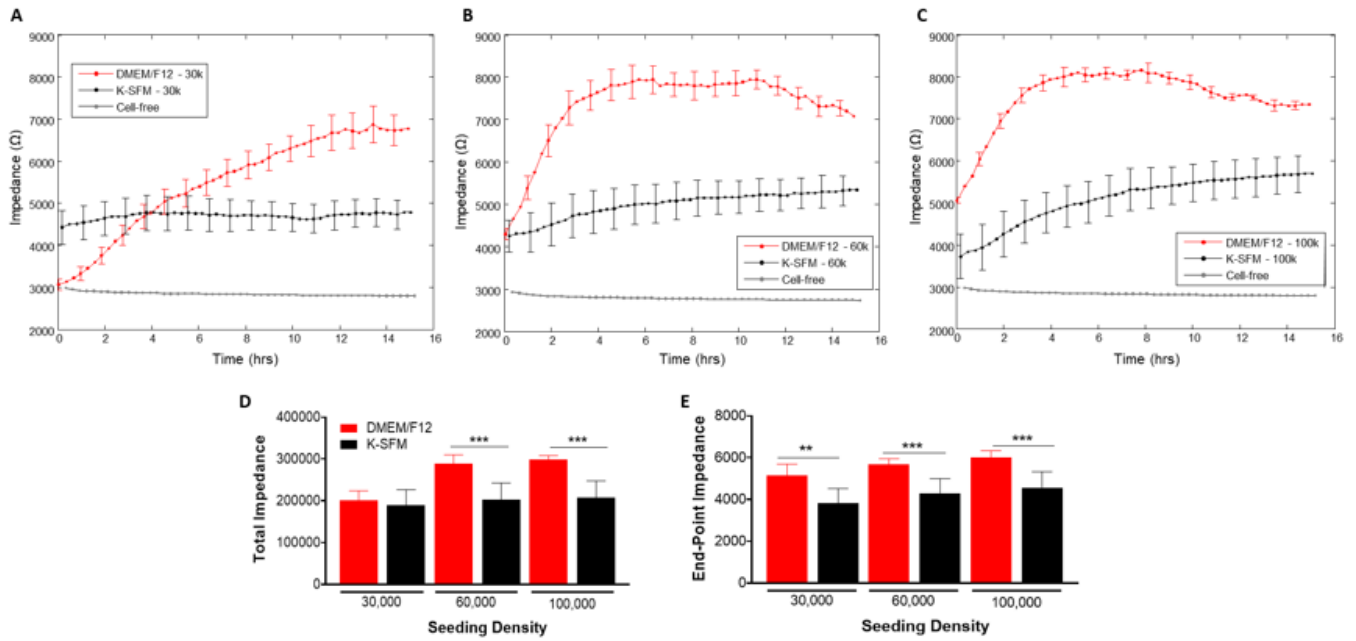


**Figure 3**

Real-time monitoring of HUCL impedance in DMEM/F12 versus K-SFM media. Impedance of HUCLs versus time, measured at an AC frequency of 32 kHz for 30,000 (**A**), 60,000 (**B**) and 100,000 (**C**) seeding densities is shown. Bar graph representation of total impedance (**D**) and end-point impedance (**E**) comparing DMEM/F12 versus K-SFM. Data shown are the mean  $\pm$  SEM;  $n = 5/\text{group}$ .  $**p \leq 0.01$  and  $***p \leq 0.001$ .

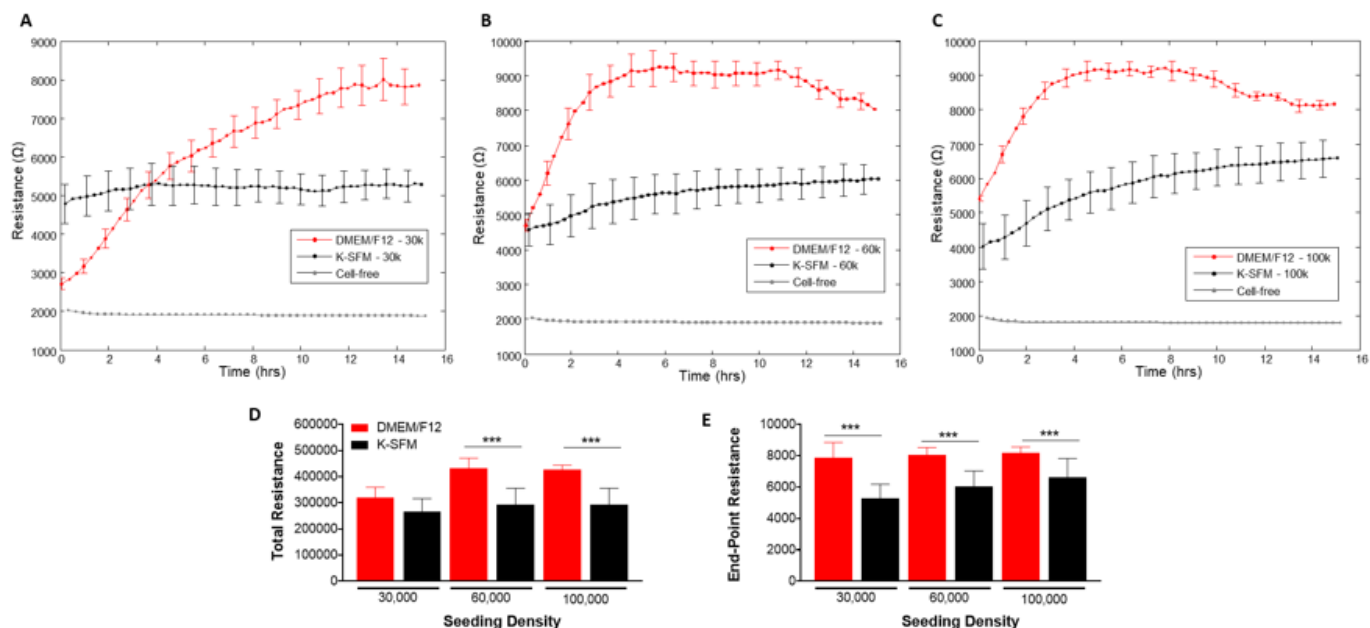


**Figure 4**

Real-time monitoring of HUCL resistance in DMEM/F12 versus K-SFM media. Resistance of HUCLs versus time, measured at an AC frequency of 4000 Hz for 30,000 (**A**), 60,000 (**B**) and 100,000 (**C**) cell seeding densities is shown. Bar graph representation of total resistance (**D**) and end-point resistance (**E**) comparing DMEM/F12 vs. K-SFM. Time = 0 hour denotes time of inoculation. Data shown are the mean  $\pm$  SEM;  $n = 5/\text{group}$ . \*\*\* $p \leq 0.001$ .

**Figure 5**

Real-time monitoring of HUCL capacitance in DMEM/F12 versus K-SFM media. Capacitance of HUCLs versus time, measured at an AC frequency of 64 kHz is shown for 30,000 (**A**), 60,000 (**B**), and 100,000 (**C**) cell seeding density. Total capacitance (**D**) and end-point capacitance (**E**) comparing DMEM/F12 vs. K-SFM are represented by bar graphs. Data shown are the mean  $\pm$  SEM;  $n = 5/\text{group}$ . \*\* $p \leq 0.01$  and \*\*\* $p \leq 0.001$ .

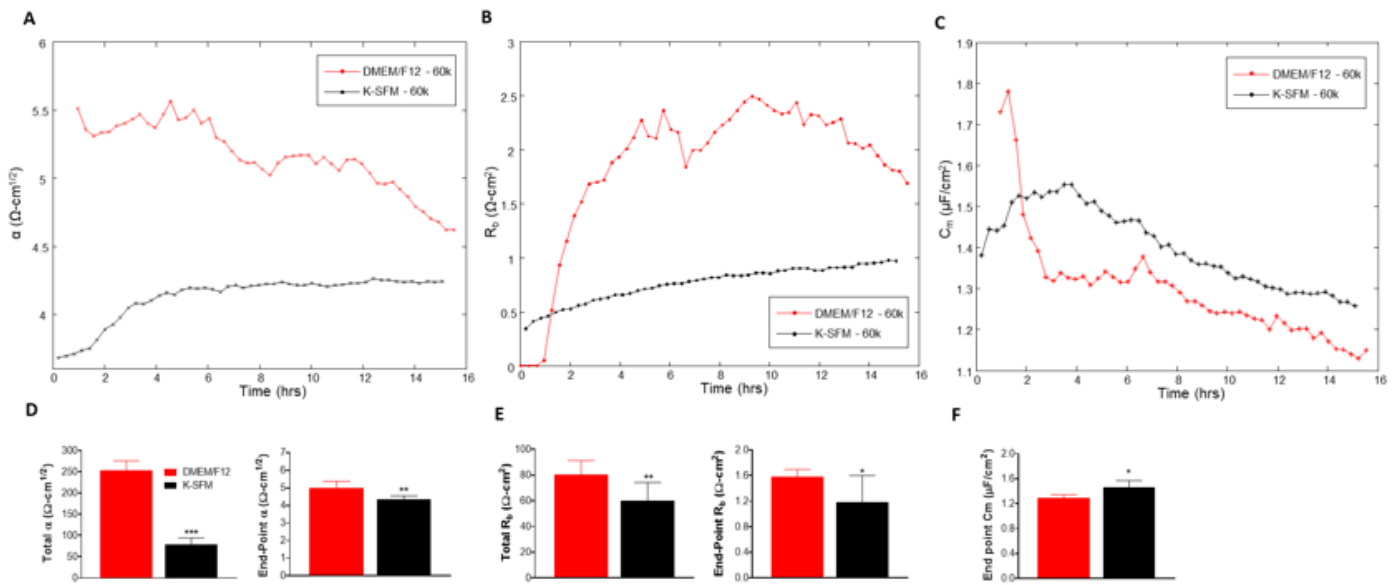


**Figure 6**

Mathematical modeling of  $\alpha$ ,  $R_b$ , and  $C_m$  for HUCLs grown in DMEM/F12 versus K-SFM media. Modeled parameters,  $\alpha$  (A),  $R_b$  (B), and  $C_m$  (C) were traced over 15 hours for cells seeded at 60,000. Time = 0 denotes time of inoculation. Bar graphs represent total and end-point values from DMEM/F12 versus K-SFM media for  $\alpha$  (D) and  $R_b$  (E); end-point only is shown for  $C_m$  (F). Data shown are the mean  $\pm$  SEM;  $n = 5/\text{group}$ . \* $p \leq 0.05$ , \*\* $p \leq 0.01$  and \*\*\* $p \leq 0.001$ .

## Supplementary Files

This is a list of supplementary files associated with this preprint. Click to download.

- [SupplementalFigure1..pdf](#)